



Published in final edited form as:

Adv Mater. 2011 November 16; 23(43): 5098–5103. doi:10.1002/adma.201103349.

Physically Associated Synthetic Hydrogels with Long-Term Covalent Stabilization for Cell Culture and Stem Cell Transplantation

Jianjun Zhang^{1,4}, Talar Tokatlian¹, Jin Zhong², Quinn KT Ng¹, Michaela Patterson³, Bill Lowry³, S. Thomas Carmichael², and Tatiana Segura^{1,*}

¹Department of Chemical and Biomolecular Engineering, University of California, Los Angeles, CA 90095, USA

²Department of Neurology, University of California, Los Angeles, CA 90095, USA

³Department of Molecular, Cell and Developmental Biology, University of California, Los Angeles, CA 90095, USA

Keywords

PEG-PPS; Amphiphilic Branched Copolymer; Self-Assembling; Injectable Hydrogel; Stem Cell Transplantation

Although the natural extracellular matrix (ECM) is primarily a self-assembled structure, a large emphasis has been placed in recent years on the development of covalently crosslinked hydrogel scaffolds for tissue regeneration and stem cell transplantation. These hydrogels allow for cell spreading and migration through cell-mediated protease degradation [1, 2] or hydrolytic hydrogel degradation [3, 4]. However, *in vivo* cells do not always migrate and spread following matrix degradation; cells are able to navigate through protein fibers [5, 6]. Further, the requirement of matrix degradation to achieve cell migration and spreading results in a change in the mechanical properties of these hydrogels with time, which makes it challenging to decouple chemical cues from mechanical cues. Hydrogel materials that can mimic non-protease mediated cell spreading and migration and do not require active matrix degradation to achieve these cellular processes can offer an alternative system to study stem cell differentiation *in vitro* and overcome some of the current limitations of purely covalently crosslinked hydrogels.

Alternatives to purely covalently crosslinked gels are physically assembled hydrogels. Physically assembled hydrogels generally yield slower gel times and do not necessarily require matrix degradation to allow cellular infiltration and spreading. In addition they are generally fluid like, allowing for delivery through injection. A variety of semi-synthetic and synthetic physically assembled hydrogels have previously been developed, including commercially available Puramatrix, other peptide based hydrogel systems [7-11], expressed protein systems [12, 13] and pluronic F-127 systems [14-16]. One limitation with physically assembled hydrogels is achieving robust mechanical properties, requiring large amount of

*Corresponding-Author Prof. Tatiana Segura 420 Westwood Plaza, 5531 Boelter Hall Los Angeles, CA 90095 tsegura@ucla.edu
Phone: +1-310-206-3980 Fax: +1-310-206-4170 .

⁴Beijing University of Chemical Technology, Beijing 100029, PR China (current location)

Additional Information

Supplemental figures S1-6 and all materials and methods can be found in the Supporting Information.

polymer for sufficient mechanical stiffness. To overcome this limitation physical crosslinks can be introduced to stabilize the self-assembled structure. However, these covalent crosslinks typically require the addition of an external trigger to induce gelation (e.g. chemical crosslinkers) after the self-assembled structure is formed, which is not always possible.

Herein we report on a non-protease degradable injectable hydrogel that uses physical association between amphiphilic branched poly(ethylene glycol)-poly(propylene sulfide) (PEG-PPS) block copolymers to form a self-assembled hydrogel network and a pyridine dithione functional group at the end of each self assembling block to further stabilize the network *in situ* by slow-forming covalent bonds. This hydrogel allows for cell spreading and proliferation *in vitro* and can be used as a vehicle for stem cell transplantation into the brain *in vivo*.

Hydrophobically-grafted poly(ethylene glycol) (PEG) has previously been investigated for the application of drug delivery vehicles such as microparticles, nanoparticles, and vesicular polymersomes [17-19]. In our laboratory, we are using four-arm PEG as a water-soluble polymer backbone with poly(propylene sulfide) (PPS) as a hydrophobic component and 2,2-dipyridine dithione as the end-capping agent to synthesize a PEG-PPS amphiphilic branched copolymer terminated with a protected disulfide (Figure 1). This synthesized PEG-PPS branched copolymer formed a flowing network through physical association of the hydrophobic PPS blocks in water, and further formed stronger hydrogels via disulfide exchange reaction of the pyridine dithione groups under physiological conditions resulting in covalent crosslinks. The end pyridine dithione groups were also utilized to modify the polymer with the integrin binding peptide Ac-GCGYGRGDSPG-NH₂ (RGD) through the same mechanism. The PEG-PPS-RGD hydrogel was suitable for *in vitro* cell culture, showing cell spreading and proliferation for mouse fibroblasts, mesenchymal stem cells and human neural progenitor cells, and for *in vivo* cell transplantation in the brain, showing enhanced stem cell survival.

Four-arm PEG-PPS branched copolymer was synthesized using anionic polymerization of propylene sulfide, as was previously done for PEG-PPS block co-polymers [20]. After each synthesis and purification step, the intermediate product was characterized with ¹H NMR (Figure S1-3) to confirm the composition and degree of modification. Based on the ¹H NMR for the final PEG-PPS product, 96% of the PEG arms were modified with PPS polymer, with 5 PPS units per PEG arm (i.e. (PEG₁₁₃-PPS₅)₄ referred to as PEG-PPS). A disulfide exchange reaction was then used to conjugate the cell adhesion peptide, RGD, to a fraction of the arms to produce PEG-PPS-RGD (Figure 1a, S4). TEM images (Figure 1b) verified that in dilute aqueous solution (0.1%) PEG-PPS copolymers were able to self-assemble into micelles with a uniform particle size of 20-30nm [21].

In determining which copolymer concentration would be suitable to form a bulk phase hydrogel, various concentrations were tested. Visually (Figure 2a) it was clear that a 1% PEG-PPS aqueous solution (pH = 6.0) still had high fluid properties. With increasing copolymer concentration, PEG-PPS showed increased viscosity (sol-gel transition) due to the strong tendency of its hydrophobic PPS blocks to physically associate. For those gels made directly in NaHCO₃ (pH 9.3), the authors hypothesize the disulfide exchange became the primary mechanism for crosslinking the gel (the pK_a of 2-pyridine dithione is 6.5) and the hydrogel quickly fell out of solution (Figure 2b). 3% PEG-PPS possessed suitable fluid properties to be injected by a syringe, while still showing network properties (no flow under gravity, Figure 2a,c). The viscoelastic properties of physical PEG-PPS hydrogels at different copolymer concentrations were found to be a function of copolymer concentration and viscosity was shown to decrease with increasing shear, indicating a shear-thinning fluid

(Figure S5). Increasing the copolymer concentration also caused both the storage (G') and loss moduli (G'') to increase as well as the difference between them, verifying that the increased sol-gel transition was a direct result of the increasing copolymer content (Figure 2d). For 3.33% hydrogels the storage modulus was found to be significantly larger than the loss modulus, which is indicative of an elastic rather than viscous material. Additionally, physically associated PEG-PPS hydrogels maintained their viscoelastic properties in water and were injectable even days after being formed, highlighting its long-term storage potential.

After incubating PEG-PPS hydrogels in the presence of NIH3T3 cells in complete cell medium (cDMEM = DMEM + 10% serum) for 336 hours, both the storage and loss moduli increased significantly ($p < 0.01$, Figure 2e,f), suggesting that further cross-linking occurred within the hydrogel to induce a transition from weaker ($G' = 10$ to 100Pa) gels to stiffer gels ($G' \sim 1000\text{Pa}$). The hydrogels were initially dissolved in milliQ water ($\text{pH} = 5.0-6.0$), which would have slow disulfide exchange reactions. When the physically crosslinked hydrogel is placed in PBS or cDMEM with cells at $\text{pH} = 7.4$ the rate of disulfide exchange increased, leading to stiffening of the gels with time. In order to further investigate the transition process, we choose 2.66% copolymer hydrogels as a model to test mechanical properties with respect to time in the presence of cells (Figure 2g,h). We found that this hydrogel began with a G' of 30Pa , which became 100Pa 12 hours later and reached a plateau at 1000Pa by 72 hours. The timescale for change showed that the transition to a stronger gel was gradual, taking several days to reach its final state. Thus, although the mechanical properties of PEG-PPS hydrogels changed for the initial 3-days of incubation with cells (increased in storage modulus), the mechanical properties did not change further between 3 and 14 days of incubation.

To demonstrate that the transition in gel strength was a direct result of disulfide crosslinks, the hydrogels were treated with a reducing agent, dithiothreitol (DTT). Immediately after addition of DTT, the storage and loss moduli decreased and continued to decrease with time (Figure 2i) until the initial physical hydrogel properties were achieved. This suggested that the transition in gel strength was caused by disulfides that formed by exchange of terminated disulfides already within each PEG-PPS arm. Together these results suggest PEG-PPS branched copolymers can form hydrogels by physical association of PPS units in an aqueous phase without external triggers, and can further form stronger physical-chemical hydrogels via disulfide exchange reaction under physiological conditions.

Thus, synthetic non-protease degradable PEG-PPS hydrogels gel in two stages: first self-assembly through hydrophobic interactions, and second by covalent crosslinking upon exposure to physiological pH due to disulfide exchange reactions between PPS units, resulting in a solid hydrogel that no longer flows. This mechanism of gelation is consistent with the observed increase in effective network chain density (ν_0) and decrease in the average molecular weight of the polymer chain between cross-linking points (M_c) upon covalent crosslinking [22] (Table S1). PEG-PPS hydrogels are also able to degrade by two separate mechanisms. Both reduction of the disulfide bonds, as demonstrated by weakening of the gel in the presence of DTT, and oxidation of the PPS units can lead to degradation of the gel (Figure S6).

To evaluate the potential use of PEG-PPS as a 3-dimensional cell matrix, mouse fibroblasts (NIH/3T3) and mouse mesenchymal stem cells (mMSCs) were chosen as cellular models. Live-dead staining on NIH/3T3 cells was initially performed to assess the cell viability inside the hydrogels after culturing for 4 and 14 days (Figure 3a). Spindle-shaped cells were able to spread in PEG-PPS hydrogels that contained RGD peptide (Figure 3a) and, conversely, were unable to spread in those hydrogels that did not contain RGD. NIH/3T3

cells remained viable over the 14-day period, as indicated by the absence of red cells. Spreading was a direct result of the hydrogel's mechanical properties, with cells spreading more in 2.66% gels than in 2% gels with identical RGD concentrations (Figure 3a). However, compared with 2.66% gels, NIH/3T3 cells spread significantly less in 3.33% hydrogels after 14 days of incubation. This trend suggested that after incubation in cell medium, 3.33% hydrogels became too stiff for cell growth, leading to cellular aggregation over time. Similar spreading of mMSCs was also observed in 2.66% hydrogels (Figure 3b). This result is significant and novel since current self-assembled hydrogels do not generally allow for extensive cell spreading in 3-dimensions and protease degradable crosslinks are required for spreading to occur in covalently crosslinked gels [1, 2, 23]. Based on our network structural analysis of the rheology data the M_c for covalently stabilized PEG-PSS hydrogels is much larger than what it would be for a purely covalently crosslink network of the same molecular weight PEG (5000 g/mol vs, 66,500 g/mol). This indicates that the cells either have enough space to spread due to pores existing within the hydrogel or are able to move the PEG-PPS polymers, generating pores suitable for cell spreading. However, hydrogel mechanical properties were not significantly affected by the culture of cells with gels retaining their elastic and storage modulus throughout the two-week incubation period, indicating that hydrogel degradation was not extensive.

To further characterize the proliferation of NIH/3T3 inside the PEG-PPS hydrogels, AlamarBlue assay was performed. The results indicated that the cellular metabolic activity continued to increase for at least 14 days (Figure 3c). However, similarly to the decline seen in spreading in 3.33% hydrogels from 2.66% hydrogels, the overall metabolic activity in 3.33% hydrogels was much lower and even decreased from 7 to 14 days (Figure 3d). This was most likely a result of increased disulfide formation with time that led to stiffening of the gel (Figure 2f), eventually adversely affecting cellular metabolic activity. Once again, similar metabolic activity of mMSCs was observed over time in 2.66% hydrogels (Figure 3e) compared to NIH/3T3 cells. Together the trends seen in survival, spreading, and metabolic activity of these two cell types indicate that, in general, 2.66% PEG-PPS hydrogels can be used effectively to culture cells *in vitro* without the requirement for degradable crosslinks. In addition this data suggest that the components of the hydrogel are non-toxic. However, detailed toxicity studies of the released 2-pyridine dithione have not been performed here and will have to be performed to move this material forward.

Given the hydrogel's effect in supporting the survival of mMSCs in culture, its effect on human induced pluripotent stem-neural progenitor cell (iPS-NPC) survival was further investigated *in vivo*. The transplantation of stem cells for applications in tissue engineering and regenerative medicine is becoming a reality [24, 25]. The major challenge facing this field is to develop an efficient system to deliver cells and promote their survival, engraftment and differentiation [26-29]. Covalently crosslinked injectable hydrogels have been extensively explored as cell delivery systems with the advantage that cells and biomolecules can be readily integrated into the gelling matrix [7, 30, 31]. Additionally, *in situ* polymerization of injectable hydrogels inherently allows for strong physical integration of the scaffold into any defect and facilitates the use of minimally invasive approaches for materials delivery. Yet, purely covalently crosslinked injectable hydrogels used to deliver stem cells *in vivo* are limited by their rapid gel time and their requirement for external triggers to induce gelation [32-33].

Specifically, the transplantation of neural progenitor stem cells into the brain has been shown to result in differentiation into neurons or glia and integration into the host tissue and enhance endogenous repair processes, such as axonal sprouting, neurogenesis and angiogenesis [27]. However, the effect is limited as most cells die when injected directly into the brain [34]. It was recently shown that the added physical support of an injectable

biopolymer hydrogel within the stroke cavity increased the survival of transplanted embryonic stem cell derived neural progenitor cells (NPCs) 2-fold [27]. In our studies iPS-NPC survival and spreading was first evaluated in 2.66% PEG-PPS hydrogels *in vitro* (Figure 4a) and determined to be comparable to that previously seen for NIH/3T3 and mMSCs. They were then transplanted with either PBS or within 2% PEG-PPS hydrogels into the brain of naive mice (Figure 4b). Fourteen days after the transplantation, survival of iPS-NPCs was evaluated. As shown in Figures 4c-d, iPS-NPCs identified with human nuclei (HuNu) staining were observed throughout the PEG-PPS hydrogel. Cell counting of HuNu stained cells indicated 1.2% (n=3) of injected iPS-NPCs survived within the hydrogel in comparison to no detectable surviving cells (n=3) when injected with PBS. Interestingly, the PEG-PPS hydrogel was able to form a barrier, which limited the infiltration of activated astrocytes identified by GFAP staining (Figure 4d), which are generally regarded as one of the causes for stem cell death following transplantation. This is unlike what was previously seen for biopolymer hydrogels *in vivo* [27]. Conversely, activated microglia (i.e. macrophages) identified by Iba1 and endothelial cells identified by PECAM staining were able to infiltrate the hydrogel (Figure 4e) and enhance stem cell survival through vascularization even without the addition of pro-angiogenic factors. Activated microglia have previously been shown to provide a strong angiogenic response *in vivo* [35]. Although cellular infiltration into the PEG-PPS hydrogel occurred, these studies do not address the optimal degradation kinetics of the hydrogel to achieve maximal stem cell survival, vascularization and functional recovery. To begin to address this question an alternative control was performed where iPS-NPCs were transplanted within covalently crosslinked protease degradable hyaluronic acid hydrogels. However, due to the severity of protease expression in the brain after transplantation the hydrogel was completely degraded after 14 days and transplanted cells could not be detected (data not shown). Therefore, it seems undesirable to have enzymatic degradation when the protease expression within the target tissue is very high. From these data we hypothesize that a slow degrading hydrogel would offer more protection to the transplanted cells and provide longer lasting mechanical support to infiltrating cells than fast degrading hydrogels. Nevertheless, the behavior of PEG-PPS hydrogels *in vivo* is unique and deserves further investigation in the future to truly understand its mechanism of action and be able to better design hydrogel scaffolds for stem cell transplantation and regeneration. Combined these results demonstrate the potential use of injectable PEG-PPS hydrogels to promote iPS-NPC survival and possible further applications to induce vascularization *in vivo*.

As presented, a novel non-protease degradable injectable hydrogel scaffold using a fully synthetic and chemically defined amphiphilic branched copolymer has been developed which is suitable for cell culture both *in vitro* and *in vivo*. PEG-PPS can self-assemble through physical association of the PPS units into a hydrogel and remain a viscoelastic solution until further crosslinking is induced by incubation under physiological conditions. The terminal disulfide group also has potential to be used as a means to incorporate functional biomolecules or peptides. PEG-PPS gels allowed for long-term culture and spreading of various cell types *in vitro*, unlike previous reports for other synthetic hydrogel systems [10, 23]. We used stem cell delivery to the brain as a model system and showed that PEG-PPS hydrogels can be used effectively as an injectable biomaterial to deliver neural progenitor stem cells and promote their survival. In addition, PEG-PPS allowed for angiogenesis, while selectively inhibiting astrocyte infiltration, unlike previously reported for hydrogel systems for this implant site [27]. This hydrogel system can further be used for a variety of other tissue engineering and regeneration applications, with the added potential of being able to incorporate desired signals, including proteins, growth factors, and DNA.

Supplementary Material

Refer to Web version on PubMed Central for supplementary material.

Acknowledgments

The authors thank Shiva Gojgini and Jonathan Lam and undergraduate researcher Priscilla Williams for their help with this project. This work was supported by the National Institutes of Health (TS R21EB007730 and TS R21EB009516) and the National Science Foundation (TS 0747539).

Appendix

Materials and methods

Materials

Sodium hydride (NaH), allyl bromide, thioacetic acid, 2,2'-azobisisobutyronitrile, sodium methoxide (NaOMe), propylene sulfide, and 2,2'-dithiodipyridine were purchased from Sigma-Aldrich (St Louis, MO). Four-arm poly(ethylene glycol) (PEG) (MW: 20000) was purchased from NEKTAR Transforming Therapeutics. RGD peptide (Ac-GCGWGRGDSPG-NH₂) was purchased from Genscript. All other chemicals were purchased from Fisher Scientific unless otherwise noted.

PEG-allyl ether synthesis

20g (4mmol arms) of four-arm PEG (20kD) was dissolved in 400mL of tetrahydrofuran (THF) in a 500mL two-neck round bottom flask and dried for 4 hours by reflux distillation (90°C) through a Soxhlet extractor filled with activated molecular sieves. To the cooled PEG solution, a total of 1.2g of NaH (8x excess over arms = 32mmol) was added to generate the alcoholate. The mixture was stirred for 15 min, and then cooled down on ice. Using an additional funnel, 4.48g (10x excess over arms = 40mmol) of allyl bromide dissolved in 6mL dichloromethane was gradually added to the reaction mixture. The solvent was then refluxed overnight. The remaining NaH was filtered using Whatman filter paper, and the volume of the solution was reduced to ~20mL using rotary evaporation. To precipitate the product, the solution was added to 500mL of cold diethyl ether, and the precipitate was filtered off and redissolved in dichloromethane. This solution was again precipitated in 500mL cold diethyl ether, after which the product was collected and dried under vacuum. NMR was used to characterize the final sample for modification. ¹H-NMR (in CDCl₃): δ=3.39-3.89 (broad, PEG chain protons), 5.85-5.98 (m, 1H, -CH₂OCH₂CH=CH₂), 5.15-5.30 (m, 2H, -CH₂OCH₂CH=CH₂) (Figure S1).

PEG-thioacetate synthesis

3.67g (0.73mmol arms) of PEG-allyl was dissolved in 130mL toluene (degassed 15 min by sonication) in a 250mL Schlenk tube. 1.5g (0.009mol) of 2,2'-Azobisisobutyronitrile (AIBN) was dissolved in the PEG solution. The solution was further degassed by argon purging for 30 min. The neck of the Schlenk tube was then stoppered with a septum. The reaction solution was stirred at 70°C. At the same time, 3mL (0.039mol) thioacetic acid and 1.5g (0.009mol) AIBN dissolved in 20mL toluene was added using a syringe. The entire volume was added in 5 separate aliquots. The addition was repeated every 2 to 3 hours. After the last addition, the reaction was carried on for a total of 72 hours. The volume of the solution was reduced to about 20mL using rotary evaporation. Precipitation and characterization of the product was carried out exactly as was done for PEG-allyl acetate. ¹H-NMR (in CDCl₃): δ=1.81-1.9 (q, 2H, -OCH₂CH₂CH₂S-), 2.35 (s, 3H, -SCOCH₃), 2.92-2.97 (t, 2H, -OCH₂CH₂CH₂S-), 3.39-3.89 (broad, PEG chain protons) (Figure S2).

PEG-PPS synthesis

0.78g of PEG-thioacetate (0.156mmol) was dissolved in 80mL of THF in a 100mL Schlenk tube, and then further degassed by argon purging for 30 min to ensure that the entire system was under argon and dry. The THF had been previously stored with molecular sieves in order to ensure it was dry. A rubber septum was placed on top of the Schlenk tube. All reagents were added via syringe. 450 μ L of NaOMe (0.5M methanol solution) was added into the reaction system, and then the reaction solution was stirred for 30 min at room temperature. Further, 61 μ L of propylene sulfide (PPS) dissolved in 2mL of degassed THF was added into the reaction system, and the solution was further stirred for 90 min at room temperature. Lastly, 176mg of dipyridine dithione dissolved in 2mL of degassed THF was added into the reaction system to end-cap the reaction. The product solution was passed through a filter cake in order to remove excess salts, and then the solution was evaporated by rotary evaporation in order to dry it as much as possible. 10mL of methanol was added to dissolve the product, and then the methanol solution was incubated in liquid nitrogen. After crystallization occurred the excess methanol was removed and the procedure was repeated 4 times. The collected product was then kept in a vacuum oven overnight. NMR was used to characterize the final product. $^1\text{H-NMR}$ (in CDCl_3): δ =1.35-1.45 (d, CH_3 in PPS chain), 1.81-1.9 (broad q, 2H, - $\text{OCH}_2\text{CH}_2\text{CH}_2\text{S}$), 3.6-3.7 (broad PEG chain protons) (Figure S3).

PEG-PPS-RGD synthesis

The cellular adhesion peptide, Ac-GCGWGRGDSPG- NH_2 (RGD), was bound to the PEG-PPS-pyridylidithione polymers using a disulfide exchange reaction between the disulfide end-capped PEG-PPS and the cysteine residue of the peptide. 20mg PEG-PPS was dissolved in 1.8mL of DI H_2O , and then diluted with 2mL of PBS buffer. 200 μ L (5mg/mL) of RGD was added to the PEG- PPS solution slowly while stirring and further reacted for 1 hr. The course of the reaction was monitored following the release of 2-pyridine dithione at 342nm (Figure S4).

Rheology analysis

PEG-PPS copolymer was dissolved in milliQ H_2O to form physically associated hydrogels with final polymer concentrations of 2, 2.66, and 3.33 %. Further, 100 μ L 2.66 % physical hydrogels were incubated in cDMEM in the presence of NIH3T3 cells (see Encapsulation of Cells in 3D protocol below) for 12, 72, and 168 hours to form physical-chemical hydrogels. The physical-chemical hydrogel transition was investigated using a strain-controlled rheometer (Physica MCR Anton Paar) with a parallel plate under a constant strain of 0.05 and frequency ranging from 0.1 to 10rad/s. Hydrogels were cut using a 6.0mm biopsy punch to fit the plate and place on top of sandpaper to prevent slipping. A humid hood was also used to prevent drying and maintain a constant temperature of 25 $^\circ\text{C}$ during testing.

Hydrogel morphologies

Morphologies of PEG-PPS hydrogels were visualized by scanning electron microscopy (SEM). The hydrogels were immersed into liquid nitrogen and freeze-dried. The dried hydrogels were gold-coated using a sputterer and visualized using a JEOL JSM-6700 FE-SEM.

Cell culture

All cell culture supplies were purchased from Invitrogen unless otherwise noted. Mouse fibroblast cells (NIH/3T3) and mouse mesenchymal stem cells (mMSCs) were purchased from ATCC (Manassas, VA, USA) and cultured in DMEM (Sigma-Aldrich) medium supplemented with 10% bovine growth serum (BGS, Hyclone, Logan, Utah) and 1% penicillin/streptomycin at 37 $^\circ\text{C}$ and 5% CO_2 . The cells were passaged using trypsin

following standard protocols. Induced pluripotent stem cells (iPS-NPCs) were donated by the Lowry lab and cultured in DMEM/F-12 (50/50) with B-27, N-2, FGF, EGF in the presence of primocin and 1% penicillin/streptomycin at 37°C and 5% CO₂. iPS-NPCs were split using 20% TrypLE.

Encapsulation of cells in 3D PEG-PPS hydrogels

60,000 cells were encapsulated into 160μL (2, 2.66, and 3.33%) PEG-PPS hydrogels with a final concentration of 200μM PEG-PPS-RGD and 150mM NaCl. Cell viability in the PEG-PPS hydrogels was studied with the LIVE/DEAD viability/cytotoxicity kit (Molecular Probes, Eugene, OR) using the manufacturer's protocol. Each gel was stained with 100μL of the staining solution for 30 min at 37°C in the dark and imaged with a confocal microscope (Leica TCS SP2 AOBS). An AlamarBlue assay was performed in order to quantify the cellular metabolic activity inside the hydrogels. 20μL of AlamarBlue dye with 100μL phenol red free DMEM was added to each well and incubated at 37°C for 4 hours. The metabolic activity was monitored at 2, 4, 8, and 14 days.

In vivo transplantation of iPS-NPCs cells

All procedures were performed in accordance with the National Institutes of Health Animal Protection Guidelines and approved by the UCLA Chancellor's Animal Research Committee. 2-month-old male C57BL/6 mice (Charles River Laboratories, Wilmington, MA) were anesthetized with 5% isoflurane and maintained with 2.5% isoflurane in N₂O:O₂ (2:1). A midline skin incision was made after the mice were placed in the stereotactic apparatus. A burr hole was drilled on the skull at 0.88mm anterior and 2mm lateral left of the bregma. iPS-NPCs cells were mixed with 2% PEG-PPS hydrogels containing 200μM PEG-PPS-RGD or PBS (8000 cells/μL). The 4μL cell mixture (cells with or without gel) was then injected stereotactically with a 30-gauge needle and 25ml Hamilton syringe at a depth of 2.8mm from the surface of the brain at a rate of 1μL/min. The needle was left in place for an additional 5 min after the injection before withdrawal. Cyclosporin A (IP 4 mg/kg daily) was used as to suppress the immune response.

Immunohistochemistry and microscopy

2 weeks post injection, mice were deeply anesthetized and perfused with buffered saline and then 4% paraformaldehyde, cryoprotected, and frozen-sectioned. Brains were cut in 6 parallel sections of 40mm thickness. Each section was then cut into 10 separate 400μm sections. Immunohistochemistry was performed as described. Briefly, brain sections were rinsed with phosphate-buffered saline blocked in normal donkey serum plus Triton- X100. Brain sections were then incubated overnight at 4°C with primary antibodies. Secondary antibodies from the appropriate hosts conjugated to cyanine 2, cyanine 3, and cyanine 5 (Jackson ImmunoResearch, West Grove, PA) were used. Sections were then counterstained with the nuclear marker DAPI (4',6-diamidino-2-phenylindole). Primary antibodies were used as follows: goat anti-doublecortin (DCX; C18, 1:500; Santa Cruz Biotechnology, Santa Cruz, CA); rat anti-platelet endothelial cell adhesion molecule-1 (PECAM-1; 1:300; BD PharMingen, San Diego, CA); rabbit anti-GFAP (glial fibrillary acidic protein) (1:1000; Zymed, San Francisco, CA); rabbit anti-Iba1 (1:400, Wako Chemicals USA, Richmond, VA). Transplanted iPS-NPCs cells were identified by anti-human nuclei antibody (HuNu; 1:400, Millipore, Billerica, MA). Imaging was done using fluorescence microscopy (ZEISS Observer. Z1).

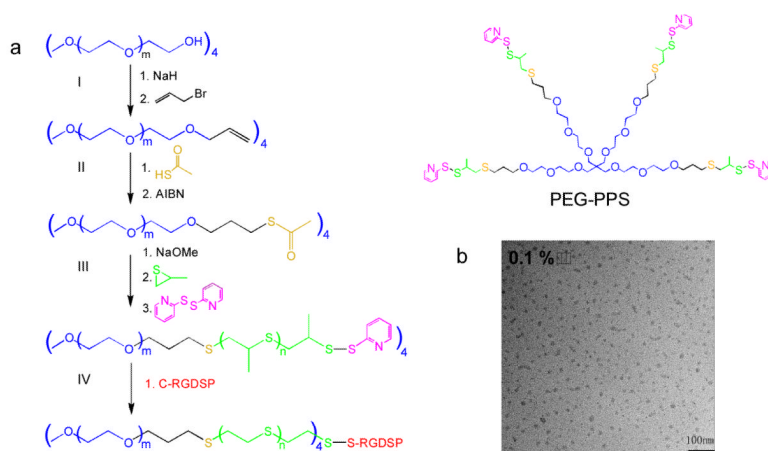
Statistics

All statistical analysis was performed using InStat (GraphPad, San Diego, CA). Experiments were statistically analyzed using the Tukey test to compare all pairs of columns using a 95% confidence interval.

References

- [1]. Lei Y, Gojgini S, Lam J, Segura T. *Biomaterials*. 2010; 32:39. [PubMed: 20933268]
- [2]. Lutolf MP, Lauer-Fields JL, Schmoekel HG, Metters AT, Weber FE, Fields GB, Hubbell JA. *PNAS*. 2003; 100:5413. [PubMed: 12686696]
- [3]. Qiu Y, Lim JJ, Scott L Jr, Adams RC, Bui HT, Temenoff JS. *Acta Biomaterialia*. 2011; 7:959. [PubMed: 21056127]
- [4]. Sahoo S, Chung C, Khetan S, Burdick JA. *Biomacromolecules*. 2008; 9:1088. [PubMed: 18324776]
- [5]. Friedl P, Brücker E-B. *Cellular and Molecular Life Sciences*. 2000; 57:41. [PubMed: 10949580]
- [6]. Wolf K, Muller R, Borgmann S, Brocker E-B, Friedl P. *Blood*. 2003; 102:3262. [PubMed: 12855577]
- [7]. Haines-Butterick L, Rajagopal K, Branco M, Salick D, Rughani R, Pilarz M, Lamm MS, Pochan DJ, Schneider JP. *PNAS*. 2007; 104:7791. [PubMed: 17470802]
- [8]. Jung JP, Nagaraj AK, Fox EK, Rudra JS, Devgun JM, Collier JH. *Biomaterials*. 2009; 30:2400. [PubMed: 19203790]
- [9]. Luo Z, Zhao X, Zhang S. *Macromolecular Bioscience*. 2008; 8:785. [PubMed: 18546148]
- [10]. Nowak AP, Breedveld V, Pakstis L, Ozbas B, Pine DJ, Pochan D, Deming TJ. *Nature*. 2002; 417:424. [PubMed: 12024209]
- [11]. Webber MJ, Tongers J, Renault M-A, Roncalli JG, Losordo DW, Stupp SI. *Acta Biomaterialia*. 2010; 6:3. [PubMed: 19635599]
- [12]. Olsen BD, Kornfield JA, Tirrell DA. *Macromolecules*. 2010; 43:9094. [PubMed: 21221427]
- [13]. Wong Po Foo CTS, Lee JS, Mulyasmita W, Parisi-Amon A, Heilshorn SC. *PNAS*. 2009; 106:22067. [PubMed: 20007785]
- [14]. Cortiella J, Nichols JE, Kojima K, Bonassar LJ, Dargon P, Roy AK, Vacant MP, Niles JA, Vacanti CA. *Tissue Engineering*. 2006; 12:1213. [PubMed: 16771635]
- [15]. Thonhoff JR, Lou DI, Jordan PM, Zhao X, Wu P. *Brain Research*. 2008; 1187:42. [PubMed: 18021754]
- [16]. Vashi AV, Keramidaris E, Abberton KM, Morrison WA, Wilson JL, O'Connor AJ, Cooper-White JJ, Thompson EW. *Biomaterials*. 2008; 29:573. [PubMed: 17980905]
- [17]. Kim SH, Tan JPK, Fukushima K, Nederberg F, Yang YY, Waymouth RM, Hedrick JL. *Biomaterials*. 2011; 32:5505. [PubMed: 21529935]
- [18]. Napoli A, Tirelli N, Wehrli E, Hubbell JA. *Langmuir*. 2002; 18:8324.
- [19]. Valencia PM, Hanewich-Hollatz MH, Gao W, Karim F, Langer R, Karnik R, Farokhzad OC. *Biomaterials*. 2011; 32:6226. [PubMed: 21658757]
- [20]. Segura T, Hubbell JA. *Bioconjugate Chemistry*. 2007; 18:736. [PubMed: 17358044]
- [21]. S, Cerritelli; Fontana, A.; Velluto, D.; Adrian, M.; Dubochet, J.; De Maria, P.; Hubbell, JA. *Macromolecules*. 2005; 38:7845.
- [22]. Jiang G-Q, Liu C, Liu X-L, Chen Q-R, Zhang G-H, Yang M, Liu F-Q. *Polymer*. 2010; 51:1507.
- [23]. Cellesi F, Weber W, Fussenegger M, Hubbell JA, Tirelli N. *Biotechnology and Bioengineering*. 2004; 88:740. [PubMed: 15532084]
- [24]. Okano H. *Proceedings of the Japan Academy, Series B*. 2010; 86:438.
- [25]. Yoshida Y, Yamanaka S. *Circulation*. 2010; 122:80. [PubMed: 20606130]
- [26]. Chai C, Leong KW. *Mol Ther*. 2007; 15:467. [PubMed: 17264853]
- [27]. Zhong J, Chan A, Morad L, Kornblum HI, Fan G, Carmichael ST. *Neurorehabilitation and Neural Repair*. 2010; 24:636. [PubMed: 20424193]
- [28]. Mooney DJ, Vandenburgh H. *Cell Stem Cell*. 2008; 2:205. [PubMed: 18371446]

- [29]. Lutolf MP, Gilbert PM, Blau HM. *Nature*. 2009; 462:433. [PubMed: 19940913]
- [30]. Hou Q, De Bank PA, Shakesheff KM. *Journal of Materials Chemistry*. 2004; 14:1915.
- [31]. Tan H, Ramirez CM, Miljkovic N, Li H, Rubin JP, Marra KG. *Biomaterials*. 2009; 30:6844. [PubMed: 19783043]
- [32]. Chiu Y-L, Chen S-C, Su C-J, Hsiao C-W, Chen Y-M, Chen H-L, Sung H-W. *Biomaterials*. 2009; 30:4877. [PubMed: 19527916]
- [33]. Xu F-J, Kang E-T, Neoh K-G. *Biomaterials*. 2006; 27:2787. [PubMed: 16442613]
- [34]. Bliss T, Guzman R, Daadi M, Steinberg GK. *Stroke*. 2007; 38:817. [PubMed: 17261746]
- [35]. Yamasaki Y, Itoyama Y, Kogure K. *Keio J Med*. 1996; 45:225. [PubMed: 8897765]

**Figure 1.**

(a) Synthetic route of four-arm PEG-PPS: (I) PEG-allyl, (II) PEG-thioacetate, (III) PEG-PPS, and (IV) PEG-PPS-RGD synthesis. (b) TEM image of $(\text{PEG}_{113}\text{-PPS}_5)_4$ self-assembled micelles at concentration of 0.1% in water at 100,000X magnification.

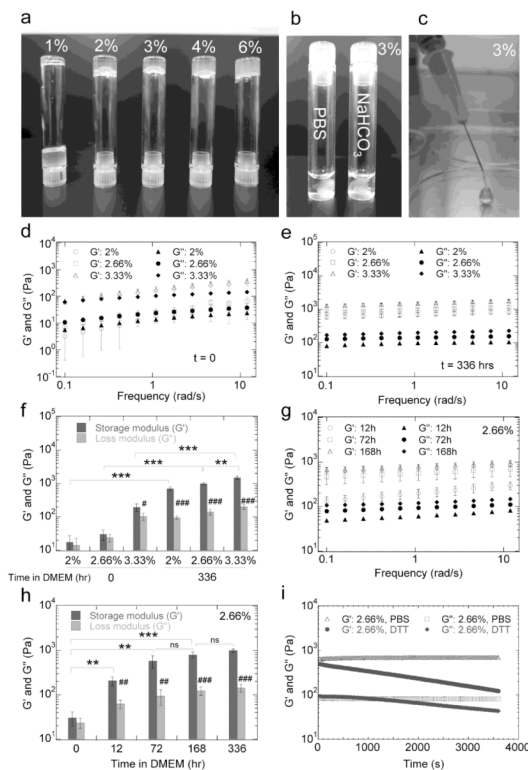


Figure 2. (a) Gelation of (PEG₁₁₃-PPS₅)₄ hydrogels at various copolymer concentrations in milliQ H₂O. (b) Gelation of 3% PEG-PPS in PBS (pH 7.4) and NaHCO₃ (pH 9.3). (c) Injectable 3% PEG-PPS hydrogels. The storage (G') and loss (G'') moduli of PEG-PPS hydrogels incubated in cDMEM in the presence of cells for 0 (d) and 336 hours (e) were analyzed to show the effect of copolymer concentration on mechanical properties. Average G' and G'' over the frequency range are shown in (g). To analyze the rate of stiffening, 2.66% gels were also incubated in cDMEM in the presence of cells for 12, 72 and 168 hours (f) with average G' and G'' shown in (h). (i) G' and G'' of 2.66% PEG-PPS hydrogels, previously incubated in cDMEM in the presence of cells for 336 hours, immediately after adding dithiothreitol (DTT) solution. The symbols ** and *** indicate significant differences of p < 0.01 and p < 0.001, respectively, and 'ns' indicates no significant difference was observed between various storage moduli. The symbols #, ##, and ### indicate significant differences of p < 0.05, p < 0.01, and p < 0.001, respectively, between the storage and loss moduli of a particular hydrogel type.

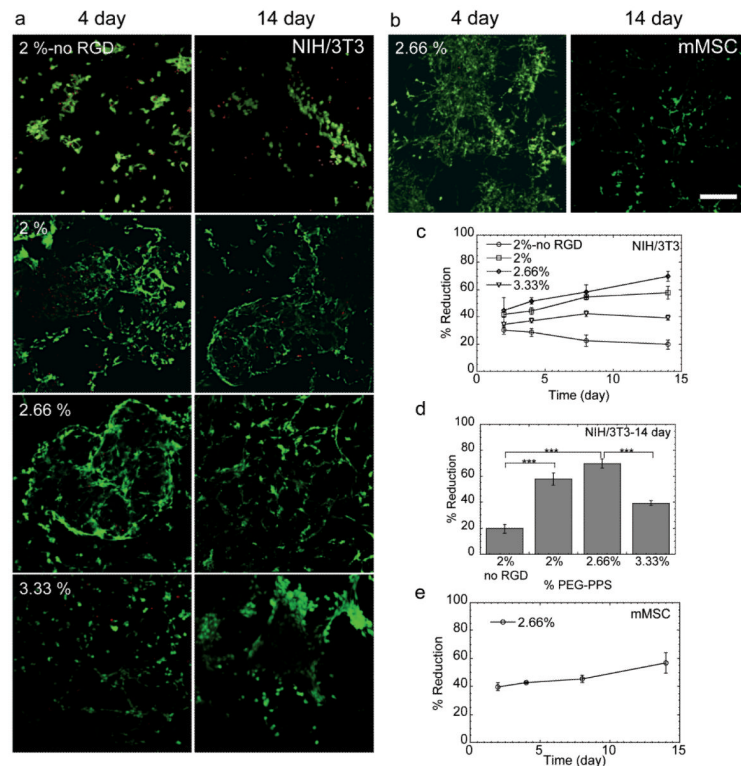


Figure 3.

(a) Live/Dead staining (green = live, red = dead) of NIH/3T3 cells in 2, 2.66 and 3.33% PEG-PPS hydrogels with and without PEG-PPS-RGD, and of (b) mMSCs in 2.66% PEG-PPS hydrogels with PEG-PPS-RGD is shown after culturing for 4 and 14 days. (c) Metabolic activity (% reduction) of NIH/3T3 cells in 2, 2.66 and 3.33% PEG-PPS hydrogels with and without PEG-PPS-RGD. Metabolic activities at 14 days are shown in (d). (e) Metabolic activity of mMSCs in 2.66% PEG-PPS hydrogels is shown over time. The symbol *** indicates a significant difference of $p < 0.001$ between various proliferation rates. Scale bar = 150 μ m.

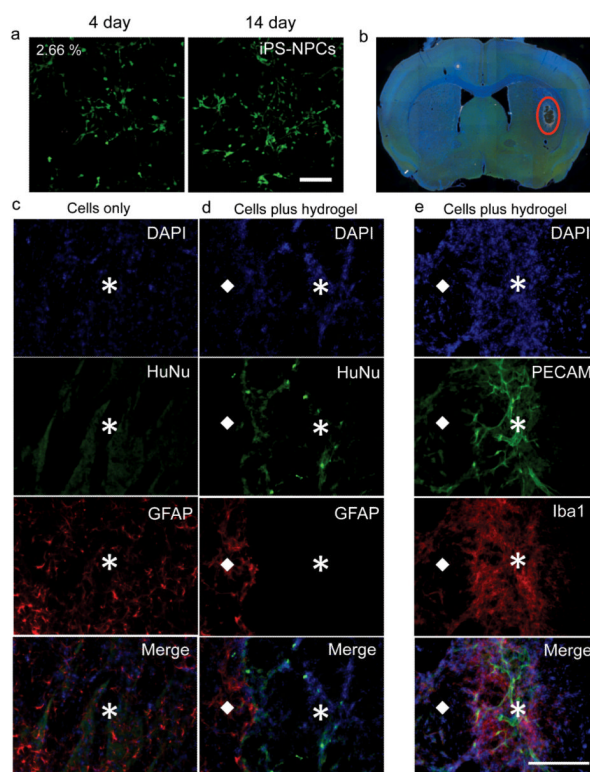


Figure 4.

(a) Live/Dead staining (green = live, red = dead) of iPS-NPCs in 2.66% PEG-PPS hydrogels is shown after culturing for 4 and 14 days. (b) Image of a mouse brain section with injected PEG-PPS (red circle). (d-c) Stained cryosections of iPS-NPCs in the hydrogel and PBS (cells only) control condition. (e) Although vascular cells infiltrated the hydrogel, the hydrogel was a barrier to astrocyte infiltration. ☒ and ◆ represent the gel area and native tissue, respectively. DAPI: nuclear stain (blue); HuNu: iPS-NPCs (green); GFAP: astrocytes (red); PECAM: endothelial cells (green); Iba 1: macrophage/microglia (red). Scale bar = 150 μm.